

## Layered Double Hydroxide Coated by Carbon-Based Material for Environmental Dye Pollutant

Neza Rahayu Palapa<sup>1,3\*</sup>, Alfian Wijaya<sup>2,3</sup>

<sup>1</sup>Department of Chemistry, Faculty of Mathematics and Natural Science, Universitas Sriwijaya, Indralaya, 30862, Indonesia

<sup>2</sup>Graduate School of Environment, Universitas Sriwijaya, Palembang, 30139, Indonesia

<sup>3</sup>Research Centre of Inorganic Chemistry and Coordination Complexes, Material Science, Universitas Sriwijaya, Palembang, 30139, Indonesia

\*Corresponding author: nezarahayu@mipa.unsri.ac.id

### Abstract

We conducted this research to modify NiAl layered double hydroxide with several carbon-based materials, including cellulose, biochar and graphite. This material was successfully prepared by coprecipitation methods and was proven by XRD, SEM, and FTIR characterization. Furthermore, we conducted the adsorption process and reusability to investigate their ability as water treatments. The dose effect on M.G. removal was investigated by the highest M.G. removal capacity using the CBC-NiAl LDHs composite, which was 100 mg. M.G. removal capacity was increased with an increase in contact time, and the saturation point was reached after 60 min for CC-NiAl and CGF-NiAl LDHs, which CBC-NiAl LDH increased and saturated after 100 min with high adsorption capacity. CC-NiAl, CBC-NiAl and CGF-NiAl LDHs composite have proved efficient, sustainable materials that maintain adsorption capability in each reusable cycle.

### Keywords

Dye Adsorption, Water Treatments, LDH Modification, Carbon-Based Material

Received: 1 September 2023, Accepted: 21 November 2023

<https://doi.org/10.26554/ijmr.20231311>

## 1. INTRODUCTION

Layered double hydroxides (LDHs) coated with carbon-based materials have shown promising potential for environmental applications (Palapa et al., 2023b), especially in the removal of dye pollutants from water (Choong et al., 2021; Mourid et al., 2019). LDHs are a class of inorganic materials with a unique layered structure consisting of positively charged metal hydroxide layers with interlayer anions to balance the charge (Sajid et al., 2022). This structure provides a high surface area and strong ion exchange capabilities, making LDHs effective adsorbents for various pollutants. However, pure LDHs may suffer from limitations such as low stability, aggregation, and slow kinetics for pollutant adsorption (Salem et al., 2022; Sajid et al., 2022). To address these issues and enhance the adsorption capacity and stability, LDHs are often coated or modified with carbon-based materials. These carbon-based materials can include graphite, graphene oxide (G.O.) (Wang et al., 2015), carbon nanotubes (CNTs) (Zhang et al., 2023), activated carbon (Alagha et al., 2020), cellulose or biochar (Li et al., 2020).

The benefits of using carbon-based materials for coating LDHs can be enhanced adsorption capacity because carbon-based materials offer additional active sites for the adsorption of dye pollutants, complementing the adsorption sites provided

by LDHs (Hakim et al., 2023). This dual functionality results in improved removal efficiency. Thus, The carbon coating acts as a protective layer for LDHs and can improve stability, preventing their aggregation and ensuring their stability during adsorption (Alagha et al., 2020; Li et al., 2020; Hakim et al., 2023; Kundu and Naskar, 2021). The synthesis of LDHs coated with carbon-based materials typically involves a two-step process. First, the LDHs are synthesized using conventional methods. Then, the carbon-based materials are deposited onto the LDH surfaces through coprecipitation, hydrothermal methods, or sol-gel techniques (Liu et al., 2020; Amin et al., 2022; Poudel et al., 2022). Combining layered double hydroxides with carbon-based materials presents a promising approach for removing environmental dye pollutants from water, offering improved adsorption efficiency, stability, and reusability compared to traditional adsorbents (Ok-triyanti et al., 2019; Chang et al., 2023). Ongoing research in this area continues to explore new materials and optimization strategies for enhanced pollutant removal and broader environmental applications.

Malachite green, a synthetic dye and antimicrobial agent of the triphenylmethane family, is used for the treatment of bacterial and parasitic diseases in aquaculture, as well as in food and textiles. Being proved harmless is its most important feature for disinfestation in aquaculture (Sharma et al., 2023). However,

malachite green contributes to environmental pollution due to its toxic effect on various organisms' organs, including animal and fish poisonings (Jaffari et al., 2023). Because of the large scale of aquaculture nowadays and using malachite green at the rates from 0.1 to 10.0% of the aquatic culture mass per day, appropriate methods for the determination of this dye and other water pollutants are extremely required (Palapa et al., 2023a).

This paper presents the necessity of including carbon-based materials between a pellet of malachite green and a carbon-coated LDH film and their application as active probes for environmental problems. Carbon-based LDH (CC, CBC and CGF) have been synthesized and applied for the adsorption of M.G. from aqueous solutions with the presence of supporting electrolytes. These materials were characterized by X-ray diffraction, scanning electron microscopy, Fourier transform infrared spectroscopy, and X-ray photoelectron spectroscopy. Their adsorption behavior was examined in dependence on the solution pH, flow rate and initial dye concentration. Adsorption isotherms were constructed from the experimental data obtained by the analysis of residual dye concentration that was determined regarding the international standard method. The surface of LDH film with homogeneous size distribution has produced many reactions toward M.G., and Dominion adsorptions were observed at the higher dye concentration after 240 min of contact time.

## 2. EXPERIMENTAL SECTION

### 2.1 Materials

The material for LDH synthesis, including  $\text{Ni}(\text{NO}_3)_2 \cdot 6\text{H}_2\text{O}$  and  $\text{Al}(\text{NO}_3)_3 \cdot 9\text{H}_2\text{O}$ , was purchased from Merck (Germany, 99% P.A.). Cellulose microcrystalline was bought from Sigma Aldrich (USA, 99% P.A.). Malachite Green (M.G.) as representative of cationic dye was obtained from Sigma Aldrich, respectively. The reagents used for the analysis process, such as NaOH and HCl, were purchased from Sigma Aldrich (USA, PA).

### 2.2 NiAl LDH Synthesis

Synthesis of NiAl LDH with  $\text{NO}_3^{2-}$  as the intercalated anion was pursued by the coprecipitation method, following the previously reported work Palapa et al. (2022). In brief, 30 mmol/L of  $\text{Ni}(\text{NO}_3)_2 \cdot 6\text{H}_2\text{O}$  and 10 mmol/L of  $\text{Al}(\text{NO}_3)_3 \cdot 9\text{H}_2\text{O}$  were mixed under vigorous stirring for 8 hours, followed by adding 40 mmol/L of NaOH until pH 10. The mixture was stirred for 30 min before heating at 80°C for 24 h. The obtained white precipitate was separated by filtration using a Whatman Filter paper and rinsed with 500 mL distilled water. The collected white solid material (NiAl- $\text{NO}_3$  LDH) was dried in an oven at 60°C for 24 h.

### 2.3 Synthesis of C-NiAl Composite

The prepared NiAl LDH was first dissolved in 250 mL of distilled water under vigorous stirring until a homogenous slurry was achieved. Then, the carbon materials (cellulose, biochar and graphite), as reported by Siregar et al. (2021), were added in each container named CC-NiAl; CBC-NiAl; and CGF-NiAl, and the stirring process was continued for 3 h. The NiAl LDH to carbon materials ratio has been set up 50:50 wt% to optimize

the obtained composite. After the mixture was homogenous, it was separated by filtration then dried in a vacuum oven at 60°C for 8 h. The obtained gray-colored material was collected and labeled as CC-NiAl LDH, The obtained black-colored material was collected and labeled as CBC-NiAl LDH and CGF-NiAl LDH.

### 2.4 Materials Characterization

The crystallinity of the synthesized materials was analyzed by X-ray diffraction (XRD) using Rigaku Smartlab equipped with Cu K-alpha radiation. The measurement was conducted from 10° to 80° with a 5°/min scanning speed. Fourier analyzed the chemical functional group in the materials transform infrared spectrometer (FTIR). The analysis was performed in Jasco FT/IR 4200 using the KBr pellet method. The sample was scanned at the wavenumber range of 4000-400 nm. The surface morphological image of the synthesized material was observed using a scanning electron microscope (SEM) (Hitachi SU8010, Japan). The surface characteristic of specific surface area and porosity of the materials was determined with  $\text{N}_2$  adsorption-desorption analysis in a Quantachrome Nova 4200e instrument. The value of the specific surface area was calculated by Branauer-Emmett-Teller (BET) method, and the pore size distribution was determined based on the Barrett-Joyner-Halenda (BJH) method. The thermal stability of the synthesized material was assessed by thermogravimetry analysis and differential thermal analysis (TG-DTA) in a Shimadzu TGA instrument.

### 2.5 Adsorption Experiments

Several factors were considered to investigate the adsorption parameters, including the mass of adsorbents, adsorption time, concentration, and temperature. The adsorption experiments were conducted using different amounts of adsorbent (ranging from 0.01 g to 0.1 g), contact periods varying from 0 to 250 minutes, initial concentrations of M.G. ranging from 10 mg/L to 30 mg/L, and reaction temperatures between 30°C and 60°C. After adsorption, the filtrate concentration was measured at a wavelength of 619 nm using a UV-Visible spectrophotometer.

## 3. RESULTS AND DISCUSSION

The XRD pattern of synthesized materials is presented in Figure 1. For comparison, the XRD pattern of NiAl LDH, carbon materials precursor, was also presented in Figure 1a. The XRD pattern of NiAl LDH exhibited sharp and symmetrical peaks at a low diffraction angle ( $2\theta$ ), confirming the successful synthesis of LDH. Moreover, the recorded diffraction pattern fit well with the JCPDS No. 35-0964, the typical hydroxylated diffraction pattern (Machrouhi et al., 2023). The primary characteristic peaks of cellulose (CC) in an XRD pattern are often observed at approximately  $2\theta$  values of 16°, 22°, and 34°. These peaks correspond to the (200), (101), and (004) crystallographic planes of cellulose, respectively. The pristine biochar (CBC) XRD pattern exhibited a broad diffraction peak at the  $2\theta$  values of 22°, which was derived from the crystalline structure of cellulose that partially remained. Taher et al. (2023) reported that the crystalline structure of cellulose has high thermal stability up

to 300°C. In the higher temperature, its main peak broadened, indicating the collapse in crystallinity and aromatic structure formation. The (002) peak in the graphite (CGF) XRD pattern is observed at approximately  $2\theta = 26.5^\circ$ . This peak is a strong and sharp reflection, indicating the high degree of order and alignment of carbon atoms within the graphite structure. NiAl LDH successfully coats and intercalates into the cellulose structure, the peaks may observe changes in the intensity and position of certain peaks compared to the pure cellulose or NiAl LDH patterns. An amorphous hump in the XRD pattern of CC-NiAl LDH. The presence of graphite (CGF) loaded into NiAl LDH caused the intensity of LDH's peak was decrease and the graphite peak around  $26.5^\circ$ , indicating the stacking of graphene layers with low intensity depended pristine one (Khajeh et al., 2020).

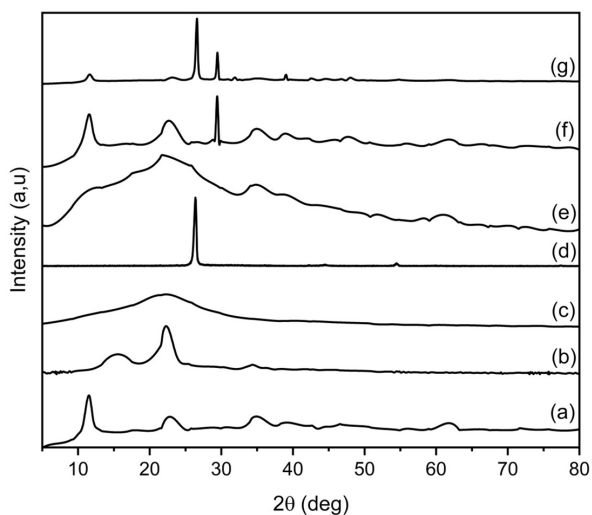


**Figure 1.** XRD Pattern of (a) NiAl LDH, (b) Cellulose, (c) Biochar, (d) Graft, (e) CC-NiAl, (f) CBC-NiAl, and (g) CGF-NiAl

The Fourier-Transform Infrared spectroscopy (FTIR) is shown in Figure 2. FTIR technique is often employed to study the vibrational modes and functional groups present in LDHs. A broad and strong peak around  $3400\text{--}3500\text{ cm}^{-1}$  is attributed to the stretching vibrations of hydroxyl groups in the LDH layers. The exact position of this peak can vary depending on the composition and hydration of the LDH. Peaks in the  $400\text{--}600\text{ cm}^{-1}$  range are associated with the stretching vibrations of metal-oxygen bonds in the LDH structure. The exact positions of these peaks depend on the nature of the metal cations present in the LDH. A broadband around  $1630\text{--}1650\text{ cm}^{-1}$  is associated with the bending vibrations of adsorbed water, and a weaker band around  $3200\text{--}3500\text{ cm}^{-1}$  is related to the stretching vibrations of water molecules. The additional peaks corresponding to these nitrate anions may appear in  $1382\text{ cm}^{-1}$ . The most prominent peak of graphite is usually around  $1620\text{--}1660\text{ cm}^{-1}$  and corresponds to the stretching vibrations of the carbon-carbon double bonds (C=C) present in the graphene sheets. Aromatic C-C Stretching of graphite also exhibits peaks related to the stretching vibrations of carbon-carbon single bonds (C-C) in the graphene lay-

ers around  $1400\text{ cm}^{-1}$  with a major peak around  $1450\text{ cm}^{-1}$ . At lower wavenumbers (below  $1000\text{ cm}^{-1}$ ), some peaks may be related to out-of-plane bending modes of the graphene sheets. The FTIR spectrum of  $900\text{--}1200\text{ cm}^{-1}$  corresponds to the stretching vibrations of C-O and O-C-O bonds of cellulose and biochar (Barkhordari and Yadollahi, 2016). Biochar characteristic bands also presented in the range of  $1000\text{--}1200\text{ cm}^{-1}$  may be observed, corresponding to Si-O stretching vibrations.

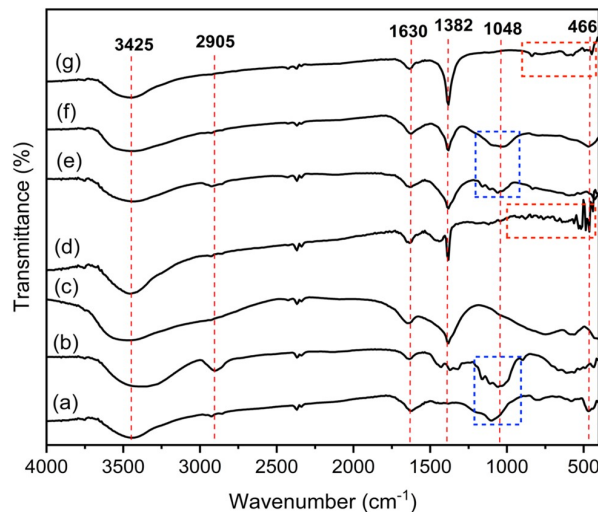


**Figure 2.** FTIR Spectra of (a) Biochar, (b) Cellulose, (c) NiAl LDH, (d) Graphite, (e) CC-NiAl, (f) CBC-NiAl, and (g) CGF-NiAl

The size, morphology, and distribution of the metal ions of NiAl LDH, CC-NiAl, CBC-NiAl and CGF-NiAl LDH have been characterized by SEM analysis. The SEM micrograph of the NiAl LDH, CC-NiAl, CBC-NiAl and CGF-NiAl LDH samples at  $10.0\text{ }\mu\text{m}$  is shown in Figure 3. In the case of the pristine NiAl LDH, the morphological properties of NiAl LDH were bulky, homogeneous, and well-developed pore crystals can provide ideal adsorption sites, as shown in (Figure 3a). Thus, the morphological properties of CC-NiAl LDH showed smoothly agglomerated structure (Figures 3b, c, and d). Conversely, the observed surface of carbon-doped NiAl LDH showed that carbon compound was well dispersed and had an almost spherical structure and more possibly demonstrated that NiAl LDHs which was strongly networked by carbon compound has developed a porous material (specifically CBC (Palapa et al., 2023b)). This observation can be explained by the formation of intermolecular interactions between carbon compound and NiAl LDHs.

From a commercial point of view, dose trials play a beneficial role for the developed model (Figure 4). The effect of dose on M.G. removal was investigated by changing the dose of the CC-NiAl, CBC-NiAl and CGF-NiAl LDHs composite from 10 to 100 mg and the results are shown in Figure 4. It was revealed that the removal capacity decreased with increasing dose of the CC-NiAl, CBC-NiAl and CGF-NiAl LDHs composite. Probably because, the active sites are saturated. Therefore it can be easier for the adsorbate to penetrate the adsorption sites. Since the highest

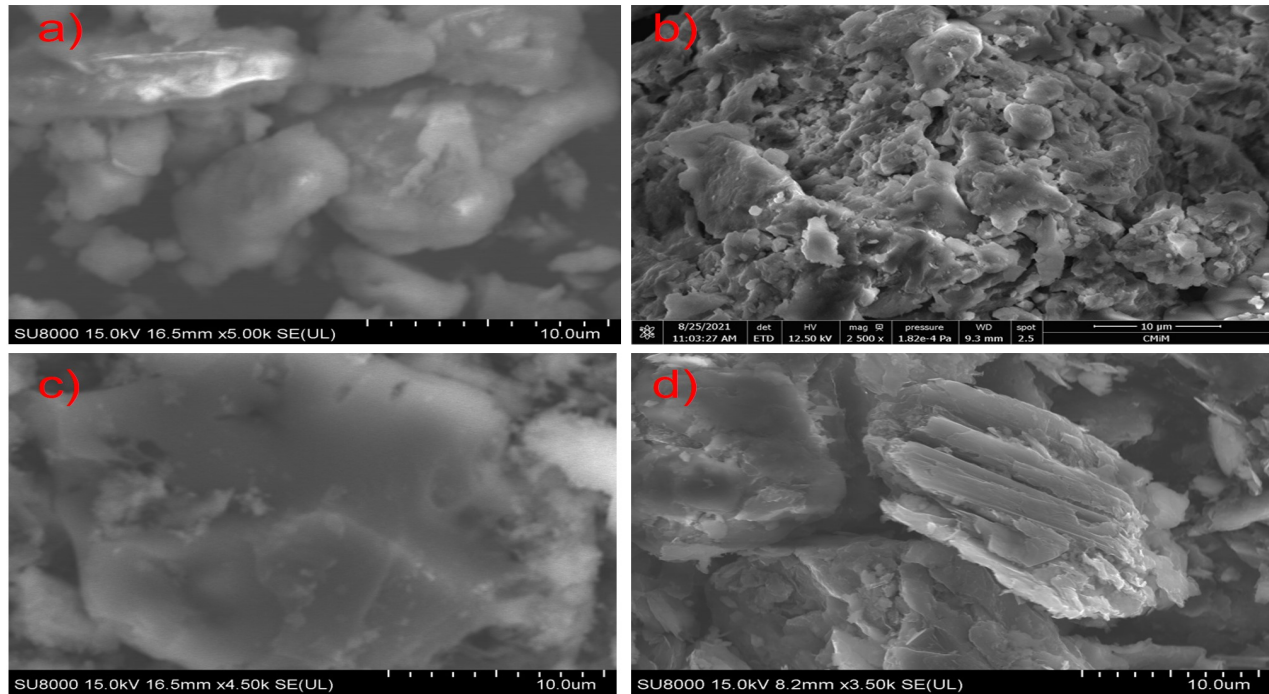


Figure 3. SEM Image of (a) NiAl LDH, (b) CC-NiAl (c)CBC-NiAl, and (d) CGF-NiAl

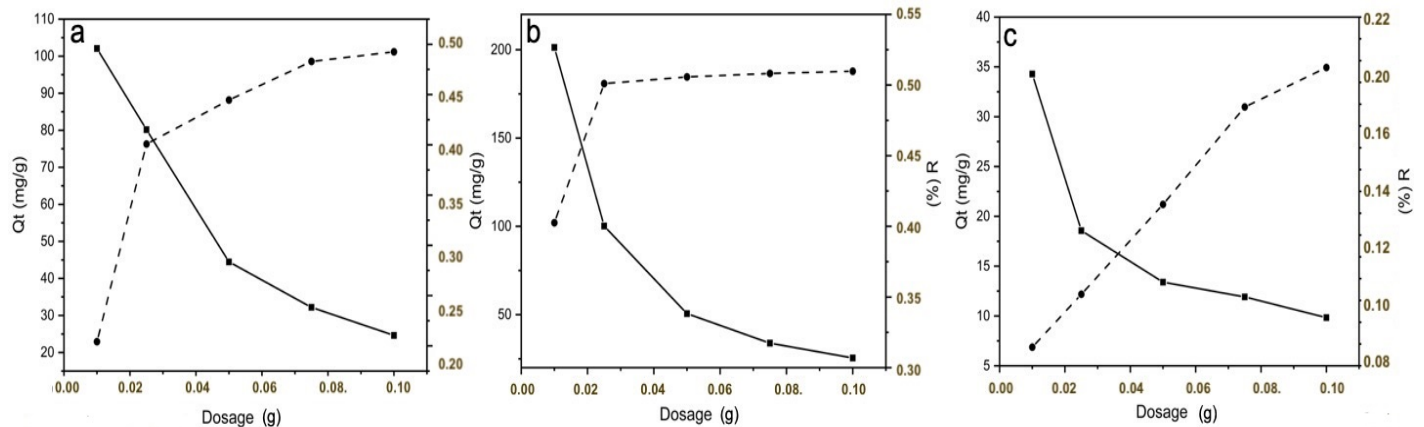


Figure 4. Adsorbent Dosage of (a) CC-NiAl (b) CBC-NiAl, and (c) CGF-NiAl

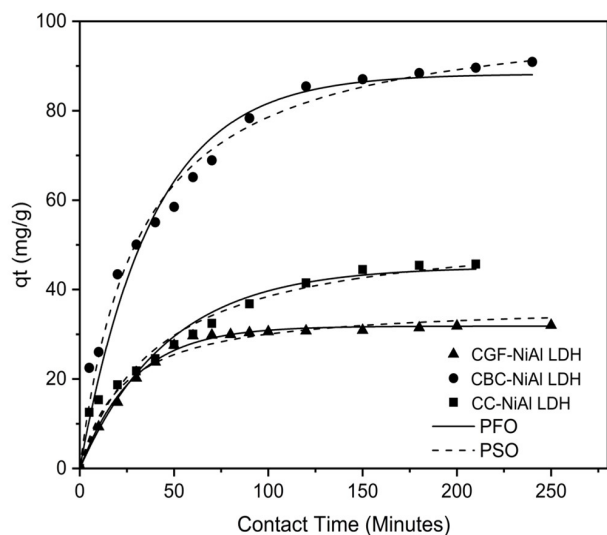
M.G. removal capacity using the CBC-NiAl LDHs composite was 100 mg, a dose of 100 mg was optimized for further experiments.

Figure 5. The effect of adsorbent contact time of composite material (CC-NiAl, CBC-NiAl, and CGF-NiAl LDHs). The effect of adsorbent contact time is one of the essential key for adsorption experiments, which can offer the lowest time required for the maximum adsorption capacity. M.G. removal capacity was increased with an increase in contact time and the saturation point was reached after 60 min for CC-NiAl and CGF-NiAl LDHs, which CBC-NiAl LDH increased and saturated after 100 min with high adsorption capacity. This phenomenon can be exposed that the number of active sites of CBC-NiAl LDHs more bigger than others composite. Therefore, in Figure 5 shows the favorability

was reached after 100 min of CBC-NiAl LDHs and no sustained changes were observed in the removal capacity of M.G. Hence, the ideal shuffling time was selected as 100 minutes for further study. From now on, the number of contact time adsorption was prepared to determine kinetic models. Experimental data were fitted to pseudo-first-order and pseudo-second-order kinetic models. Linear plots of  $(t/qt)$  for second-order models are shown in Figure 5. Second-order models' regression coefficients ( $R^2$ ) exceeded 0.99 at different initial M.G. concentrations, all higher than first-order models. Therefore, the chemisorption was the rate-controlling step for M.G. adsorption by CC-NiAl, CBC-NiAl and CGF-NiAl LDHs. Based on Figure 5, the comparison results of this research with others has been listed in Table

**Table 1.** Comparison of Common Adsorbent Materials for Removing M.G. and Its Adsorption Ability

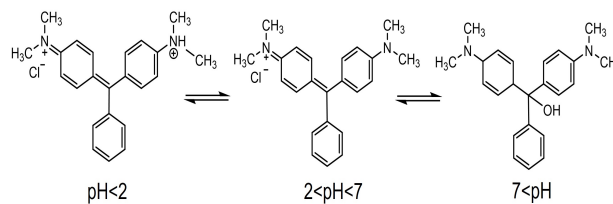
Adsorbent type	Adsorbent composition	Kinetic parameters; adsorption time (h)	Mass of adsorbent (g); Volume of adsorbate (mL); Concentration of MG (mg/L)	Kinetic adsorption capacity (mg/g)	Refs.
Carbon based materials	Coconut activated carbon	PFO; 12 h	0.05 g; 200 mL; 200 mg/L	91.24	(Qu et al., 2019)
	Chitosan-deep eutectic solvent	PSO; 20 min	0.1 g; 20 mL; 100 mg/L	17.86	(Sadiq et al., 2020)
Aerogels	Graphene oxide/aminated lignin aerogels	PSO; 12 h	0.01 g; 50 mL; 100 mg/L	63.5	(Chen et al., 2020)
Polymer matrix nanocomposites	GumT-cl-HEMA/TiO <sub>2</sub>	PSO; 80 min	0.03 g; 50 mL; 50 mg/L	11.93	(Sharma et al., 2023)
Synthetic clay	POM-CuCr LDH	PSO; 200 min	0.25 g; 25 mL; 50 mg/L	45.65	(Palapa et al., 2021)
	CC-NiAl LDH	PSO; 250 min	0.05 g; 50 mL; 100 mg/L	38.4	This research
	CBC-NiAl LDH	PSO; 200 min	0.05 g; 50 mL; 100 mg/L	92.8	This research
	CGF-NiAl LDH	PSO; 250 min	0.05 g; 50 mL; 100 mg/L	32.04	This research

**Figure 5.** The Effect of Adsorbent Contact Time and Kinetic Parameters Fitting Curves

1. According Table 1, CBC-NiAl LDH has good performance of adsorption compared common adsorbent materials for removing M.G.

The change structure formation of malachite green depend

on aqueous phase (acid-base), shown in Figure 6. The stability of M.G. showed in M.G.'s phase ( $2 < \text{pH} < 7$ ). It has been reported that the pKa value of  $\text{MG}^+$  is 6.9, and the stability pH of  $\text{MG}^+$  at 4-5 (Srivastava et al., 2004) and the dimethylamino group in  $\text{MG}^+$  is protonated at  $\text{pH} < 2$  forming  $\text{MG}^{2+}$ , while  $\text{MG}^+$  is likely to be hydrolyzed to produce carbinol ( $\text{MG}-\text{OH}$ ) at a high pH solution as shown in Figure 6. Therefore, the adsorption process using pH variations was not carried out in this research.

**Figure 6.** The Change Formation of M.G. Structure on Acid-Base Phase

The best fitted PSO kinetic model ( $R^2$  close to one), the studies indicated that monolayer chemisorption was the dominant mechanism. CC-NiAl, CBC-NiAl and CGF-NiAl LDHs composite have proved efficient sustainable materials that maintain adsorption capability in each reusable cycle. The reuse study was conducted 0.05 g of adsorbents and 50 mL M.G. solution (50

mg/L). Figure 7 shows the best performance in CBC-NiAl with the fresh adsorption of 94.2%. Apart from that, for CC-NiAl the adsorption percentage decreased drastically in the fifth cycle the adsorbent was no longer able to adsorb M.G. This is because the chemisorption process causes the adsorbent to peel off and become damaged.

Furthermore, although the CGF-NiAl LDH adsorbent's adsorptively was poor compared to CC-NiAl in the first and second cycles, CGF-NiAl showed better performance in the third to fifth cycles. although in the end reuse was only good for the first 3 cycles of M.G. adsorption. Furthermore, these materials was appropriate to treat the dyes in water.

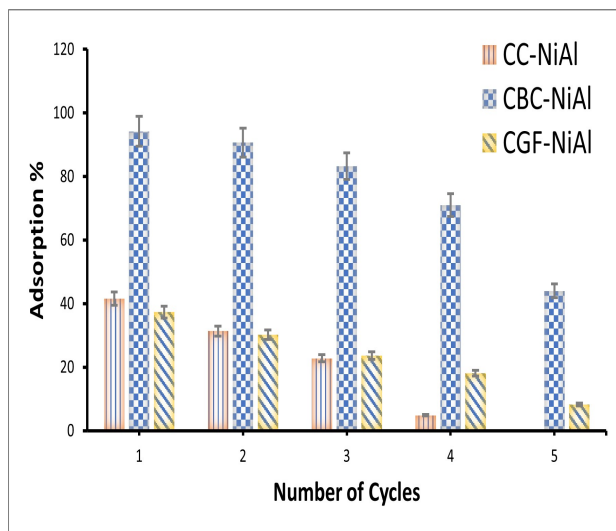


**Figure 7.** Reusability of CC-NiAl, CBC-NiAl, and CGF-NiAl for M.G. Adsorption

#### 4. CONCLUSION

Layered double hydroxides (LDHs) coated with carbon-based materials have shown promising potential for environmental applications, especially in removing dye pollutants from water. To address these issues and enhance the adsorption capacity and stability, LDHs are often coated or modified with carbon-based materials. Combining layered double hydroxides with carbon-based materials presents a promising approach for removing environmental dye pollutants from water, offering improved adsorption efficiency, stability, and reusability compared to traditional adsorbents. The surface of materials with homogeneous size distribution has produced many reactions toward M.G., and Dominion adsorptions were observed at the higher dye concentration after 240 min of contact time. The XRD pattern of NiAl LDH exhibited sharp and symmetrical peaks at a low diffraction angle ( $2\theta$ ), confirming the successful synthesis of LDH. NiAl LDH successfully coats and intercalates into the cellulose structure, the peaks may observe changes in the intensity and position of certain peaks compared to the pure cellulose or NiAl LDH patterns. The presence of graphite (CGF) loaded into NiAl LDH

caused the intensity of LDH's peak to decrease. The graphite peak was around  $26.5^\circ$ , indicating the stacking of graphene layers with low intensity depended pristine one. In the case of the pristine NiAl LDH, the morphological properties of NiAl LDH were bulky, homogeneous, and well-developed pore crystals can provide ideal adsorption sites.

Conversely, the observed surface of carbon doped NiAl LDH showed that carbon compound was well dispersed and had an almost spherical structure and more possibly demonstrated that NiAl LDHs which was strongly networked by carbon compound has developed a porous material specifically CBC. To investigate the effectivity of water treatment process, the dose effect on M.G. removal was investigated by the highest M.G. removal capacity using the CBC-NiAl LDHs composite was 100 mg. M.G. removal capacity was increased with increase in contact time and the saturation point was reached after 60 min for CC-NiAl and CGF-NiAl LDHs, which CBC-NiAl LDH increased and saturated after 100 min with high adsorption capacity. CC-NiAl, CBC-NiAl and CGF-NiAl LDHs composite have proved efficient sustainable materials which maintain adsorption capability in each reusable cycle.

#### 5. ACKNOWLEDGEMENT

The authors thank to Research Center of Inorganic Materials and Complexes Universitas Sriwijaya for valuable discussion, apparatus, and chemical analysis.

#### REFERENCES

- Alagha, O., M. S. Manzar, M. Zubair, I. Anil, N. D. Mu'azu, and A. Qureshi (2020). Magnetic Mg-Fe/LDH Intercalated Activated Carbon Composites for Nitrate and Phosphate Removal from Wastewater: Insight into Behavior and Mechanisms. *Nanomaterials*, **10**(7); 1361
- Amin, M., A. Alazba, and M. Shafiq (2022). Ldh of NiZnFe and Its Composites with Carbon Nanotubes and Data-Palm Biochar with Efficient Adsorption Capacity for Rb5 Dye from Aqueous Solutions: Isotherm, Kinetic, and Thermodynamics Studies. *Current Applied Physics*, **40**; 90–100
- Barkhordari, S. and M. Yadollahi (2016). Carboxymethyl Cellulose Capsulated Layered Double Hydroxides/Drug Nanohybrids for Cephalexin Oral Delivery. *Applied Clay Science*, **121**; 77–85
- Chang, J. H., P. Sivasubramanian, C. D. Dong, and M. Kumar (2023). Study on Adsorption of Ammonium and Nitrate in Wastewater by Modified Biochar. *Bioresource Technology Reports*, **21**; 101346
- Chen, H., T. Liu, Y. Meng, Y. Cheng, J. Lu, and H. Wang (2020). Novel Graphene Oxide/Aminated Lignin Aerogels for Enhanced Adsorption of Malachite Green in Wastewater. *Colloids and Surfaces A: Physicochemical and Engineering Aspects*, **603**; 125281
- Choong, C. E., K. T. Wong, S. B. Jang, P. Saravanan, C. Park, S.-H. Kim, B.-H. Jeon, J. Choi, Y. Yoon, and M. Jang (2021). Granular Mg-Fe Layered Double Hydroxide Prepared Using

- Dual Polymers: Insights into Synergistic Removal of As(III) and As(V). *Journal of Hazardous Materials*, **403**; 123883
- Hakim, Y. M., R. Vinsiah, and S. Fajri (2023). High Efficient of Ca/Al-Graphite for Removal of Direct Orange. *Indonesian Journal of Material Research*, **1**(1); 15–22
- Jaffari, Z. H., A. Abbas, S. M. Lam, S. Park, K. Chon, E. S. Kim, and K. H. Cho (2023). Machine Learning Approaches to Predict the Photocatalytic Performance of Bismuth Ferrite-Based Materials in the Removal of Malachite Green. *Journal of Hazardous Materials*, **442**; 130031
- Khajeh, R. T., S. Aber, and M. Zarei (2020). Comparison of NiCo<sub>2</sub>O<sub>4</sub>, CoNiAl-LDH, and CoNiAl-LDH@NiCo<sub>2</sub>O<sub>4</sub> Performances as ORR Catalysts in MFC Cathode. *Renewable Energy*, **154**; 1263–1271
- Kundu, S. and M. K. Naskar (2021). Carbon-Layered Double Hydroxide Nanocomposite for Efficient Removal of Inorganic and Organic Based Water Contaminants—Unravelling the Adsorption Mechanism. *Materials Advances*, **2**(11); 3600–3612
- Li, S., L. Dong, Z. Wei, G. Sheng, K. Du, and B. Hu (2020). Adsorption and Mechanistic Study of the Invasive Plant-Derived Biochar Functionalized with CaAl-LDH for Eu(III) in Water. *Journal of Environmental Sciences*, **96**; 127–137
- Liu, J. C., B. Qi, and Y. F. Song (2020). Engineering Polyoxometalate-Intercalated Layered Double Hydroxides for Catalytic Applications. *Dalton Transactions*, **49**(13); 3934–3941
- Machrouhi, A., M. Khnifira, W. Boumya, M. Sadiq, M. Abdenouri, A. Elhalil, F. Mahjoubi, and N. Barka (2023). Experimental and Density Functional Theory Studies of Methyl Orange Adsorption on Ni-Al/LDH Intercalated Sodium Dodecyl Sulfate. *Chemical Physics Impact*, **6**; 100214
- Mourid, E. H., M. Lakraimi, L. Benaziz, E. H. Elkhattabi, and A. Legrouri (2019). Wastewater Treatment Test by Removal of the Sulfamethoxazole Antibiotic by a Calcined Layered Double Hydroxide. *Applied Clay Science*, **168**; 87–95
- Oktriyanti, M. M., N. R. Palapa, R. Mohadi, and A. Lesbani (2019). Modification Of Zn-Cr Layered Double Hydroxide With Keggin Ion [ $\alpha$ -SiW<sub>12</sub>O<sub>40</sub>]<sup>4-</sup> As Cr(VI) Adsorbent. *Indonesian Journal of Environmental Management and Sustainability*, **3**(3); 93–99
- Palapa, N. R., P. M. S. B. N. Siregar, A. Wijaya, T. Taher, and A. Lesbani (2022). High Selectivity and Stability Structure of Layered Double Hydroxide-Biochar for Removal Cd(II). *Bulletin of Chemical Reaction Engineering & Catalysis*, **17**(3); 520–532
- Palapa, N. R., T. Taher, A. Wijaya, and A. Lesbani (2021). Modification of Cu/Cr Layered Double Hydroxide by Keggin Type Polyoxometalate As Adsorbent of Malachite Green from Aqueous Solution. *Science and Technology Indonesia*, **6**(3); 209–217
- Palapa, N. R., A. Wijaya, N. Ahmad, A. Amri, R. Mohadi, and A. Lesbani (2023a). Activated Hydrochar Prepared from Longan Fruit (*Dimocarpus longan Lour.*) Peel via Hydrothermal Carbonization-NaOH Activation for Cationic Dyes Removal. *Science and Technology Indonesia*, **8**(3); 461–470
- Palapa, N. R., A. Wijaya, P. M. S. B. N. Siregar, A. Amri, N. Ahmad, T. Taher, and A. Lesbani (2023b). Adsorption of Fe(II) by Layered Double Hydroxide Composite with Carbon-Based Material (Biochar and Graphite): Reusability and Thermodynamic Properties. *Indonesian Journal of Chemistry*, **23**(1); 101–112
- Poudel, M. B., M. Shin, and H. J. Kim (2022). Interface Engineering of MIL-88 Derived MnFe-LDH and MnFe<sub>2</sub>O<sub>3</sub> on Three-Dimensional Carbon Nanofibers for the Efficient Adsorption of Cr(VI), Pb(II), and As(III) Ions. *Separation and Purification Technology*, **287**; 120463
- Qu, W., T. Yuan, G. Yin, S. Xu, Q. Zhang, and H. Su (2019). Effect of Properties of Activated Carbon on Malachite Green Adsorption. *Fuel*, **249**; 45–53
- Sadiq, A. C., N. Y. Rahim, and F. B. M. Suah (2020). Adsorption and Desorption of Malachite Green by Using Chitosan-Deep Eutectic Solvents Beads. *International Journal of Biological Macromolecules*, **164**; 3965–3973
- Sajid, M., S. M. S. Jillani, N. Baig, and K. Alhooshani (2022). Layered Double Hydroxide-Modified Membranes for Water Treatment: Recent Advances and Prospects. *Chemosphere*, **287**; 132140
- Salem, M. A., A. M. Khan, Y. K. Manea, and A. A. Wani (2022). Nano Chromium Embedded in f-CNT Supported CoBi-LDH Nanocomposites for Selective Adsorption of Pb<sup>2+</sup> and Hazardous Organic Dyes. *Chemosphere*, **289**; 133073
- Sharma, J., S. Sharma, and V. Soni (2023). Toxicity of Malachite Green on Plants and Its Phytoremediation: A Review. *Regional Studies in Marine Science*, **62**; 102911
- Siregar, P. M. S. B. N., N. R. Palapa, A. Wijaya, E. S. Fitri, and A. Lesbani (2021). Structural Stability of Ni/Al Layered Double Hydroxide Supported on Graphite and Biochar toward Adsorption of Congo Red. *Science and Technology Indonesia*, **6**(2); 85–95
- Srivastava, S., R. Sinha, and D. Roy (2004). Toxicological Effects of Malachite Green. *Aquatic Toxicology*, **66**(3); 319–329
- Taher, T., Y. G. Wibowo, S. Maulana, N. R. Palapa, A. Rianjanu, and A. Lesbani (2023). Facile Synthesis of Biochar/layered Double Oxides Composite by One-Step Calcination for Enhanced Carbon Dioxide (CO<sub>2</sub>) Adsorption. *Materials Letters*, **338**; 134068
- Wang, J., X. Mei, L. Huang, Q. Zheng, Y. Qiao, K. Zang, S. Mao, R. Yang, Z. Zhang, Y. Gao, et al. (2015). Synthesis of Layered Double Hydroxides/Graphene Oxide Nanocomposite As a Novel High-Temperature CO<sub>2</sub> Adsorbent. *Journal of Energy Chemistry*, **24**(2); 127–137
- Zhang, D., M. Zhao, H. Zhang, M. Terrones, and Y. Wang (2023). A Novel Electro-Synthesis of Hierarchical Ni-Al LDH Nanostructures on 3D Carbon Nanotube Networks for Hybrid-Capacitors. *Carbon*, **201**; 1081–1089